Title
Flexible Blade-Coated Multicolor Polymer Light-Emitting Diodes for Optoelectronic Sensors.

Journal
Advanced materials (Deerfield Beach, Fla.), 29(22)

ISSN
0935-9648

Authors
Han, Donggeon
Khan, Yasser
Ting, Jonathan
et al.

Publication Date
2017-06-01

DOI
10.1002/adma.201606206

Peer reviewed

Flexible Blade-Coated Multicolor Polymer Light-Emitting Diodes for Optoelectronic Sensors

*Donggeon Han, Yasser Khan, Jonathan Ting, Simon M. King, Nir Yaacobi-Gross, Martin J. Humphries, Christopher J. Newsome, and Ana C. Arias**

A method to print two materials of different functionality during the same printing step is presented. In printed electronics, devices are built layer by layer and conventionally only one type of material is deposited in one pass. Here, the challenges involving printing of two emissive materials to form polymer light-emitting diodes (PLEDs) that emit light of different wavelengths without any significant changes in the device characteristics are described. The surface-energy-patterning technique is utilized to print materials in regions of interest. This technique proves beneficial in reducing the amount of ink used during blade coating and improving the reproducibility of printed films. A variety of colors (green, red, and near-infrared) are demonstrated and characterized. This is the first known attempt to print multiple materials by blade coating. These devices are further used in conjunction with a commercially available photodiode to perform blood oxygenation measurements on the wrist, where common accessories are worn. Prior to actual application, the threshold conditions for each color are discussed, in order to acquire a stable and reproducible photoplethysmogram (PPG) signal. Finally, based on the conditions, retrieved PPG and oxygenation measurements are successfully performed on the wrist with green and red PLEDs.

Organic light-emitting diodes (OLEDs) have changed the conventional paradigm of light-emitting devices and are driving innovations in optoelectronic technologies and applications. The fact that OLEDs can be made flexible makes them suitable for diverse usage, including wearable electronics.[1–3] Indeed, OLEDs have gone beyond flexible; now it is possible to stretch and crumple them, which makes OLEDs even more unique than their solid-state counterparts.[4] On par with the investment and interest, researchers have investigated OLEDs in numerous contexts, and research on solution processable polymer light-emitting diodes (PLEDs) is no exception. One of the primary advantages of PLEDs is that they can be fabricated with printing techniques. Printing PLEDs allows for reduced material consumption, low-cost mass-production, and simplified fabrication procedures as compared to conventional evaporated OLEDs or spin-coated PLEDs.[5] In fact, adopting printing schemes into the fabrication of OLED displays is considered crucial in industries to improve the cost competitiveness against conventional display technologies.[6] Also, the merits of printing PLEDs allow them to be potentially disposable, which provides numerous new opportunities. Disposable medical devices that require light sources can largely benefit by utilizing PLEDs instead of solid-state LEDs as the lifetime requirements for these devices are not as stringent as consumer electronics. Additionally, in wearable sensing scenarios, flexible devices enhance the signal-to-noise ratio (SNR) by conforming to the skin.[7–10] Due to the flexible form factor, PLEDs provide the same advantage of improved SNR by establishing a high-fidelity sensor–skin interface that improves light coupling to the skin and reduces ambient noise.

To date, several printing techniques have been introduced for PLED fabrication. Inkjet printing allows selective deposition of different kinds of polymers by controlling the ink drop rate and the substrate surface energy, which makes it a promising choice for the next generation deposition technology in display industries.[5,11] Slot-die coating is another printing technique, which can provide large area homogeneous films, and has been previously used for organic photovoltaics (OPVs) and PLEDs.[12,13] Other printing methods that have been used in electronics are screen printing,[14] gravure printing,[15] and blade coating.[16–18] Among these techniques, blade coating is especially attractive in that the blade does not directly contact the target surface, is relatively simple to configure, has high throughput, consumes low amount of material, and provides thickness control of the deposited material by tuning coating parameters. The technique has also been previously used to fabricate all-printed organic thin-film transistors (OTFTs)[19] and organic photodiodes.[20] One of the problems that blade coating has is that the deposited film demonstrates nonuniform thickness along the blade-coating direction. It was shown that it is possible to control the uniformity of the thickness by blowing hot air over the target area[17] or by using a modified blade-coating system, where a slit is placed in front of the blade to provide a constant amount of solution to the blade.[18]

Dr. D. Han, Y. Khan, J. Ting, Prof. A. C. Arias
Department of Electrical Engineering and Computer Sciences
University of California
Berkeley, CA 94720, USA
E-mail: acarias@eecs.berkeley.edu
Dr. S. M. King, Dr. N. Yaacobi-Gross, Dr. M. J. Humphries, Dr. C. J. Newsome
Cambridge Display Technology Limited
Godmanchester, Cambridgeshire PE29 2XG, UK

DOI: 10.1002/adma.201606206

For both display and sensing systems with LEDs, having a variety of colors is crucial.[21,22] In LED displays, three fundamental colors, red, green, and blue, are used to generate all other derivative colors.[5,11] In sensing systems, having multiple wavelengths broadens the extent of applications by allowing for ratiometric measurements. For example, in pulse oximetry, using a single color enables only photoplethysmogram (PPG) measurements. On the other hand, two colors, red and green, enable pulse oxygenation measurement via ratiometric sensing.[1,2] The deposition of multicolor LEDs with monolithic process, in a single substrate, reduces process steps and simplifies system integration.[6] High-resolution printing techniques have been previously used to demonstrate full color displays.[5,23] However, depositing multiple active materials with high throughput and simple coating techniques, such as blade coating, remains a challenge. More specifically, for PLEDs, only a single-color PLED per substrate has been demonstrated, limiting their usage to single-color applications.[16–18]

Recently, spin-coated PLEDs have been used to measure pulse and oxygenation, demonstrating that they can be used for optoelectronic sensing.[1,2] Red and green PLEDs, which were fabricated on separate substrates, were coupled with an organic photodiode to perform PPG measurements. Furthermore, the oxygenation measurement was performed using transmission of light through fingertips. The transmission-mode measurement technique limits the sensing locations to the extremities of the body, where light can travel through the skin and tissue. In reflection-mode sensing scheme, light emitters and detectors remain on the same side of the skin and acquire the PPG signal via reflected light.[2] With reflection-mode sensing, it is possible to go beyond conventional sensing locations. Moreover, to truly realize the full potential of PLEDs in medical applications such as pulse oximetry, it is ideal to use a high-throughput manufacturing scheme such as blade coating to fabricate the PLEDs. Here we report on multicolor blade-coated PLEDs fabricated on a flexible substrate designed to perform reflection-mode pulse oximetry on the wrist. The blade-coating area is designated by surface energy patterning (SEP). SEP has previously been used for OTFTs to print the source and drain with PEDOT:PSS in desired patterns.[19] As for the colors of PLEDs, green, red, and near-infrared (NIR) are chosen, which are colors capable of executing PPG measurements.[1,24] Blade-coated single-color PLEDs are characterized—power efficiencies of 31.2, 42.7, and 8.6 mW W^{-1} for green, red, and NIR, respectively at 1 W sr^{-1} m^{-2} are obtained. All devices were stable throughout the full characterization process and showed uniform light emission in the active area of 0.49 cm^2. We further utilize SEP to print two colors on one substrate to realize and demonstrate multicolor blade-coated PLEDs, the performance of which are similar to the single-color PLEDs. At 1000 cd m^{-2}, luminous efficacies of 12.2 and 8 lm W^{-1} for green and red are obtained, respectively. For demonstrating reflection-mode PPG measurements in conjunction with a silicon photodiode (PD), the operating condition of the PLEDs is tuned to provide adequate flux for measuring the PPG signal at the wrist. It is worth noting that a number of factors can influence the PPG signal, such as the wavelength of the light, the intensity of the light, and geometry of the device. PLED operating current-density (J_{op}) of 10 mA cm^{-2} resulted in 0.68, 0.89, and 0.19 mW of flux which provided 1.1, 1.0, and 1.2 mV PPG signals for green, red, and NIR PLEDs, respectively. Light absorption in the tissue depends on the wavelength of the light; therefore, PPG signal attenuation of visible light is more pronounced than that of NIR light.[25] The spacing between two PLEDs is designed so that a photodiode can be placed in between the PLEDs. Finally, with the fabricated multicolor PLEDs and a silicon PD, we perform reflection-mode PPG measurements on a subject's wrist to accurately record pulse and oxygenation values, which are confirmed by a commercially available transmission-mode pulse oximeter that is used on the index finger.

The blade-coating process for fabricating the PLEDs is schematically shown in **Figure 1**a,b, and the structures of single-color and multicolor PLEDs are shown in Figure 1c,d, respectively. The red structure in Figure 1a is the blade coater being pushed by an actuator (not shown in the illustration) and the two white stripes are the indium tin oxide (ITO) strips. There is a small, controllable gap underneath the blade that can be used to alter the film thickness. A hydrophobic self-assembled monolayer (SAM) is deposited on a 10 cm × 10 cm PEN/ITO substrate, which is patterned using oxygen plasma with a mask made out of Kapton tape. The desired wetting area is exposed to the oxygen plasma such that the SAM layer is etched off to perform SEP on the PEN/ITO substrates. SEP creates hydrophilic areas on the substrate where blade-coated ink adheres to, while the other regions remain hydrophobic. Regions which are hydrophobic after SEP are indicated by yellow areas in Figure 1a. Figure S1 in the Supporting Information compares the blade-coating processes with and without the SEP. When coated without the SEP, the ink spreads across the blade, seeping under the blade support at both sides. As a result, more ink is required to print the layer, and the resulting printed film exhibits poor reproducibility. When using SEP, the coated pattern remains narrower than the width of the blade support (Figure 1a). Hence, the ink is confined in the pattern and leaking through the sides is not observed, which consequently reduces the amount of ink used from 100 to 60 µL, and improves the pattern reproducibility. Incorporating SEP in blade coating also provides a relatively longer uniform printing range (≈5 cm), especially when the target thickness is around 70 nm. While it is possible to achieve reproducible thin (20–40 nm) poly(3,4-ethylenedioxythiophene)-poly(styrenesulfonate) (PEDOT:PSS) films without SEP, the blade-coating conditions need frequent adjustments, especially for a thicker layer (70 nm) of PEDOT:PSS film, which is attributed to the ink leaking mentioned above. The layer thicknesses show a continuous decrease along the blade-coating direction (Table S1, Supporting Information). By using SEP, we achieved consistent film thickness of around 70 nm in a printing range of 5 cm, which is the region 4–9 cm away from the reservoir (active region). We characterized the printed film both along and horizontal to the direction of blade coating, and confirmed that the thicknesses in the active region are homogeneous and reproducible (Table S1 and S2, Supporting Information). In Figure S3a,b in the Supporting Information, we assessed the film quality by using atomic force microscopy and an optical profiler, and the peak-to-peak roughness was less than 10 nm for both cases. Within the active region, we observed three macroscopic defects or pinholes on average, such as the one

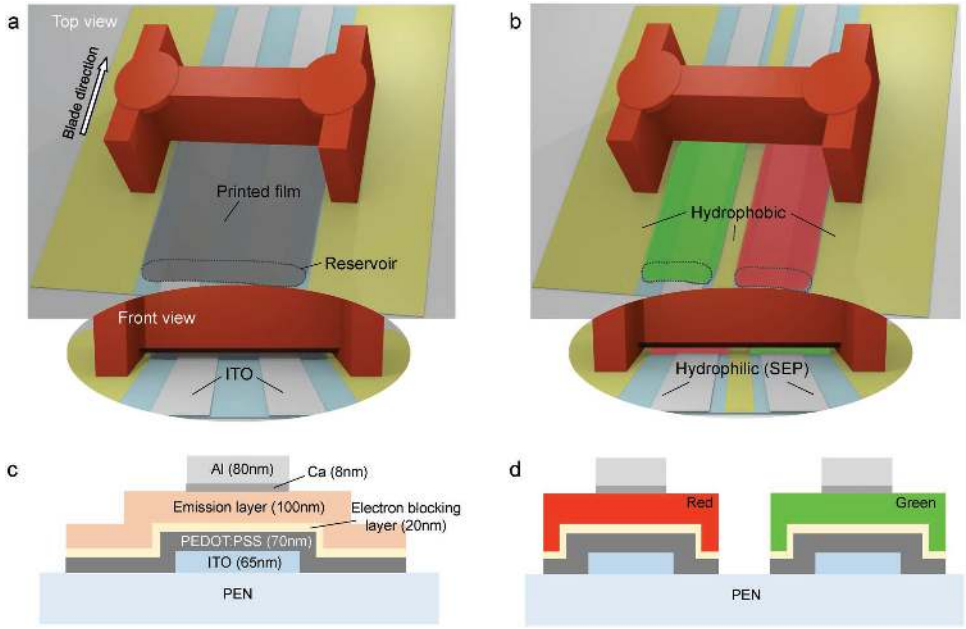

Figure 1. a,b) Illustration of top and front view of the blade-coating process using SEP for single-color PLEDs (a) and multicolor PLEDs (b). The yellow areas indicate hydrophobic regions and the dark gray dotted areas are reservoirs, where the solution is deposited prior to blade coating. c,d) PLED structures of single-color PLEDs (c) and multicolor PLEDs (d).

shown in Figure S3c (Supporting Information). However, such defects did not have much influence on the roughness near the defect (Figure S3d, Supporting Information) or on the overall film quality. Edge quality of the printed film is shown in Figure S4 (Supporting Information). The quality of the edge does not influence the device performance, because the PLED emission area is defined by the overlapping area of the ITO strip and the metal electrode. Since the blade-coated films are wider than the emission area, the edges do not influence the device performance. The same printing technique can be optimized to print well-defined edges, which was previously demonstrated for OTFTs.[19]

For multicolor PLEDs, a thin strip of Kapton tape is added in between the two ITO strips before plasma etching (Figure 1b). The solutions are then delivered separately in front of the blade, at the edges of the two sections divided by the thin Kapton tape where the blade coating starts. Two different materials can be coated utilizing this separation with a single blade-coat.

For high-quality and reproducible PLED fabrication on flexible substrates, it is crucial to have the target surface as flat as possible prior to blade coating, especially when working with thickness and roughness sensitive devices such as PLEDs. We utilize poly(ethylene naphthalate) (PEN) as the substrate and patterned ITO electrodes as the anode. The PEN/ITO is firmly attached to a glass carrier with Gel-Film (Gel-Pak). The glass/Gel-Film substrate carrier system is portable and provides a facile way to make a nonrigid substrate flat to make it convenient to handle or process. This system ensures that the substrates are planar and therefore aids a more uniform film to be deposited. One of the challenges when processing on plastic substrates is the fact that deformation occurs at temperatures near the material's glass-transition temperature (T_g). This dramatically affects the fabrication process, as any slight deformation of the surface adversely affects the quality of the solution-processed film. During the PLED fabrication, 180 °C annealing is required to activate crosslinking of the electron-blocking layer (EBL) in order to allow the subsequent deposition of the emission layer. Using the glass/Gel-Film carrier system the substrate deformation is minimized at the highest temperature used here. The samples mounted on the glass carrier with Gel-Film showed no noticeable deformation while the samples with no carrier are noticeably deformed (Figure S5, Supporting Information), increasing the challenge of depositing the subsequent layers.

Single-color PLEDs with emission in the green, red, and NIR region are fabricated using the SEP technique shown in Figure 1a. The device characterization of the single-color PLEDs is presented in **Figure 2**. The current-density–voltage–radiance (J–V–R), total flux–J, external quantum efficiency–radiance (EQE–R), and power efficiency–radiance (PE–R) characteristics are shown in Figure 2a–d, respectively. All devices show a notably clean diode behavior without abnormal discontinuities and have turn-on at less than 3 V as seen in the J–V curves (Figure 2a). Total fluxes reach up to 0.68, 0.89, and 0.19 mW at $J = 10$ mA cm^{-2} from a common emission area of 0.49 cm^2, with electroluminescence (EL) peaks at 520, 611, and 725 nm, respectively. At $R = 1$ W sr^{-1} m^{-2}, the green PLED operates at 4.6 V, with an EQE of 6.3% and PE of 31.2 mW W^{-1}, the red PLED operates at 4.5 V, with an EQE of 10% and PE of 42.7 mW W^{-1}, and the NIR PLED operates at 6 V, with an EQE of 3.1% and PE of 8.6 mW W^{-1}, respectively. Device operating voltage (V_{op}), EQE and PE in mW W^{-1} at $R = 1$ and 10 W sr^{-1} m^{-2} of each color are summarized separately in **Table 1**. Devices show stable characteristics and can provide the expected amount of flux during the course of pulse oximetry measurement. The averaged device operating voltages of 30 green, red, and NIR

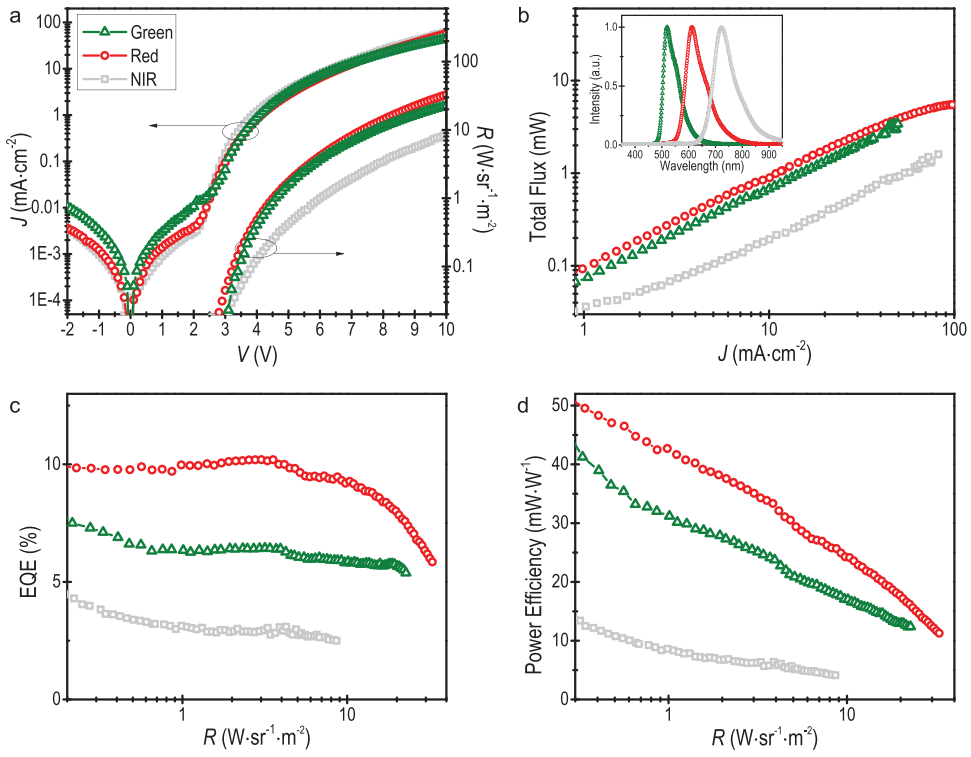

Figure 2. Device performance of single-color (green, red, and NIR) PLEDs on PEN/ITO. a) Current-density–voltage–radiance characteristics; b) total flux versus current-density; c) external quantum efficiency versus radiance; d) power efficiency (mW W^{-1}) versus radiance of each device. The inset in (b): normalized electroluminescence (EL) spectra of the three colors.

PLEDs are presented in Table S3 in the Supporting Information to highlight the reproducibility of the printing technique.

To realize multicolor PLEDs on the same substrate, we utilized the SEP technique shown in Figure 1b and fabricated green and red PLEDs on the same substrate. The specific colors are used in order to perform pulse oximetry using PLEDs.[1,2] Each PLED pixel area is 0.7 cm × 0.7 cm with 1.7 cm spacing to accommodate a photodiode in between the PLEDs. The device characterization of the multicolor PLEDs is presented in **Figure 3**. The current-density–voltage–luminance (*J*–*V*–*L*), total flux–*J*, external quantum efficiency–*L* (EQE–*L*), and luminous efficacy–*L* (LE–*L*) plots are shown in Figure 3a–d, respectively. A photograph of the multicolor PLEDs is shown in the inset picture of Figure 3c. Similar to the single-color PLEDs shown in Figure 2, the multicolor PLEDs demonstrate clean *J*–*V* characteristics and turns on at less than 3 V. The total flux and the shape of the EL spectra are equivalent to those of the single-color PLEDs. At L = 1000 cd m^{-2}, the green PLED has V_{op} of 6.1 V, EQE of 6.8%, and PE of 12.2 lm W^{-1} and the red PLED has V_{op} of 5.8 V, EQE of 11.8%, and PE of 8 lm W^{-1}. V_{op}, EQE, and PE at L = 100 and 1000 cd m^{-2} for both colors are summarized in **Table 2**. These device characteristics verify that the two different colors are successfully deposited on a single substrate, and the fabricated multicolor PLEDs are equally stable as the single-color PLEDs.

The multicolor PLEDs (green and red) are used together with a silicon PD to form an optoelectronic sensor that is placed on the wrist. The designed oximeter system is shown in **Figure 4**a. The sensor is interfaced with an analog front end (AFE), which drives the PLEDs and reads data from the PD. Two gain stages are used as shown in Figure 4b: the first gain stage amplifies both the AC and DC part of the PPG signal, and the second gain stage amplifies only the AC part of the signal. The AFE keeps track of the DC level of both the green (Gr_{DC}) and red (Rd_{DC}) channels as these are used in the pulse oxygenation calculations. The AFE sends out the PPG data to a microcontroller (μC) through a serial peripheral interface (SPI) bus. The signal is sent to a computer using a universal serial bus (USB) for processing and visualization. For applying the multicolor PLEDs as the light source in a reflection-mode pulse oximeter system, the

Table 1. Summary of V_{op}, EQE, and PE of green, red, and NIR PLEDs at radiance of 1 and 10 W sr^{-1} m^{-2}.

	@ R = 1 W sr^{-1} m^{-2}			@ R = 10 W sr^{-1} m^{-2}		
	V_{op} [V]	EQE [%]	PE [mW W^{-1}]	V_{op} [V]	EQE [%]	PE [mW W^{-1}]
Green	4.6	6.3	31.2	7.7	5.9	17.1
Red	4.5	10	42.7	7.3	9.2	24.3
NIR	6	3.1	8.6	–	–	–

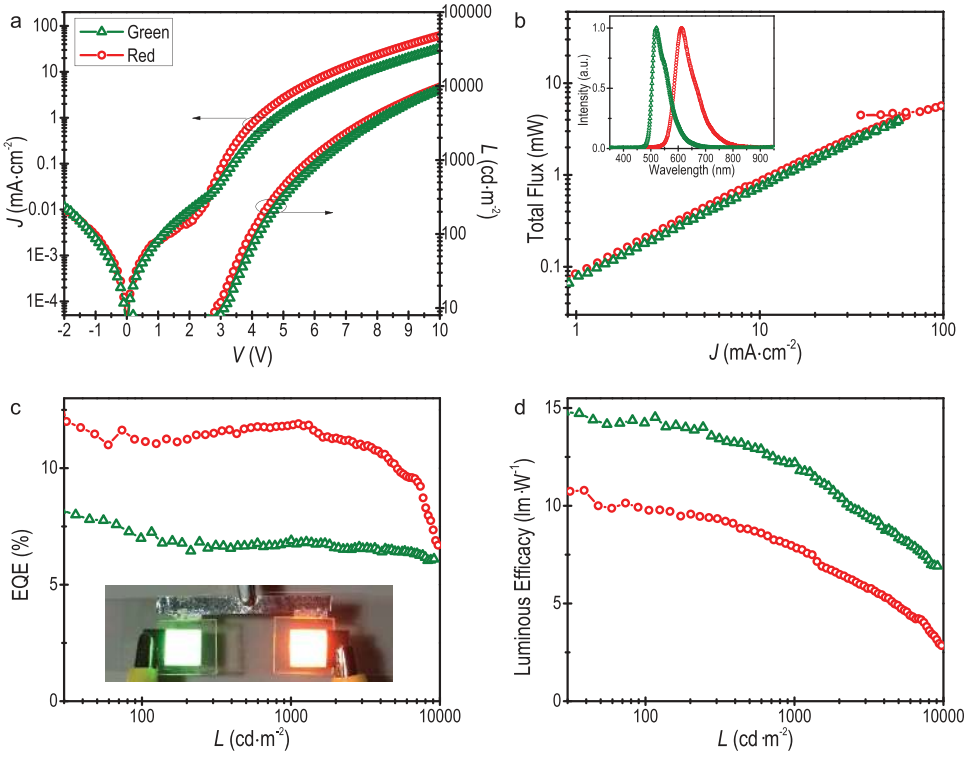

Figure 3. Device performance of multicolor PLEDs (green and red) on PEN/ITO. a) Current-density–voltage–luminance characteristics; b) total flux versus current-density; c) external quantum efficiency versus luminance; d) power efficiency (lm W^{-1}) versus luminance of each device. The inset in (b): normalized EL spectra of the two colors. The inset in (c): photograph of multicolor PLEDs in operation at 6 V.

operating conditions of the PLEDs need to be adjusted in a way such that adequate PPG signal levels are obtained during the measurement. Prior to using multicolor PLEDs for the measurement, each single-color PLED (green, red, or NIR) and a silicon PD are used to take PPG measurements, which are carried out on a volunteer's wrist. This is a typical location where watches or bracelets are worn. To the extent of our knowledge, PPG measurements on the wrist using OLEDs has not been demonstrated yet. The PPG signal intensity on the wrist is significantly smaller than the one measured from the index finger thus more challenging to acquire a strong signal. A series of PPG measurements at different PLED J_{op} using single-color PLEDs are evaluated in order to determine the optimum PLED operating conditions for acquiring the PPG signals. The pulse signal magnitudes for the different PLED driving conditions are shown using green, red, and gray colored bars in Figure 4c. Although it was possible to obtain PPG signals at J_{op} of 1, 2, and 4 mA cm^{-2}, low signal intensities hindered the reproducibility of the measurement. The PPG signals measured at 10 mA cm^{-2} were clear and reproducible for all the colors (Figure 4d–f). We observed larger signal drift in the case of NIR compared to other colors, however the signal magnitude was highest for the NIR. A peak detection algorithm is used to detect the heart rate from the PPG signals as shown in the bottom panels of Figure 4d,e. The PLEDs used for the PPG measurement are immediately characterized again to check the total flux according to J (Figure S6, Supporting Information), which are not different from their initial state (Figure 2b). By crosschecking this data with the PPG measurement, it is possible to correlate signal magnitude with total flux. 1.1, 1.0, and 1.2 mV PPG signals are obtained using 0.68, 0.89, and 0.19 mW of fluxes, respectively for green, red, and NIR PLEDs.

Finally, we perform reflection-mode pulse oximetry using the multicolor PLEDs and a silicon PD. The blade-coated multicolor PLEDs are cut horizontally so that it can be placed on the wrist. The photograph in **Figure 5**a shows the configuration of the optoelectronic sensor when placed on the wrist. The oximeter system as described above is used to simultaneously collect the PPG signals from the green and red channels. The signals are shown in Figure 5b (top two panels). Heartbeat peaks (blue dots) and valleys (red dots) are detected from the PPG signals, and the heart rate (HR) in beats per minute (b.p.m.) by timing

Table 2. Summary of V_{op}, EQE, and PE of green and red PLEDs in multicolor PLEDs at luminance of 100 and 1000 cd m^{-2}.

	@ L = 100 cd m^{-2}			@ L = 1000 cd m^{-2}		
	V_{op} [V]	EQE [%]	LE [lm W^{-1}]	V_{op} [V]	EQE [%]	LE [lm W^{-1}]
Green	4.2	7	14.2	6.1	6.8	12.2
Red	3.9	11.2	9.9	5.8	11.8	8

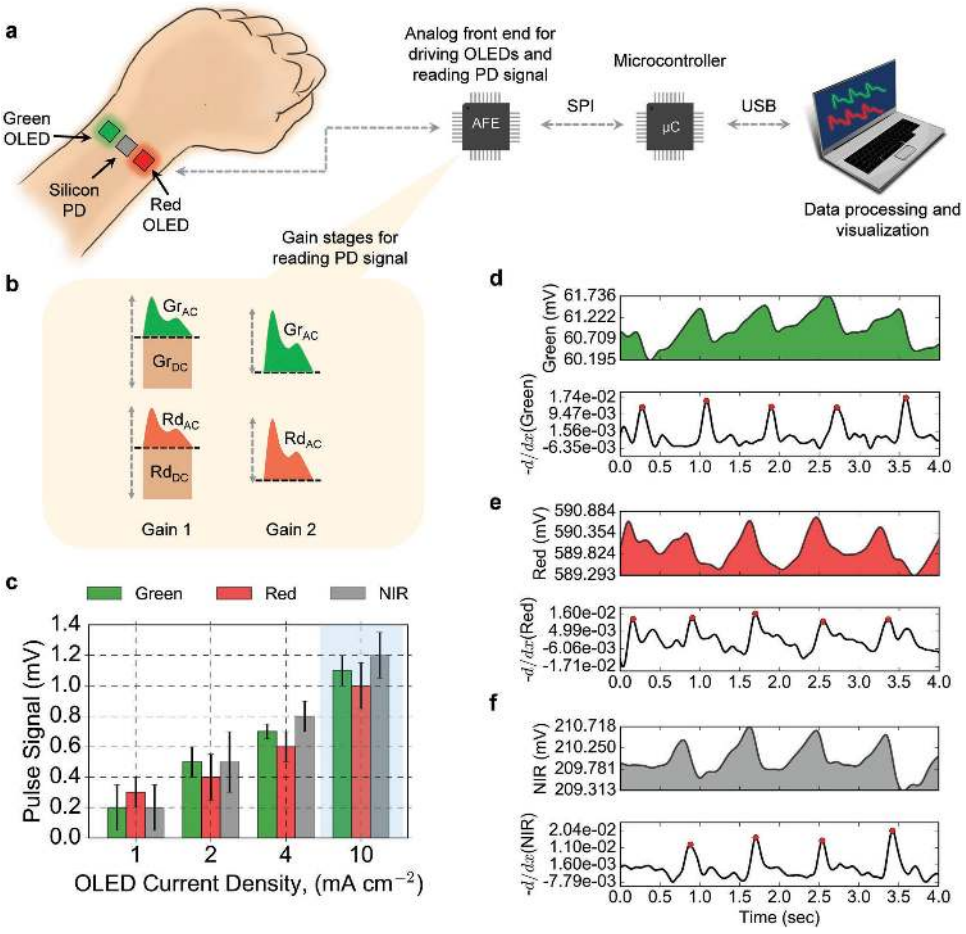

Figure 4. System design and PLED specifications for obtaining photoplethysmogram (PPG) signal from the wrist. a) Schematic illustration of the system setup for acquiring the PPG signal. An optoelectronic probe composed of green and red PLEDs, and a silicon PD are placed on top of the wrist. The PLEDs and the PD are controlled using an analog front end (AFE). The AFE filters and amplifies the PD signal and sends to a microcontroller (μC) over serial peripheral interface (SPI) bus. The processed signal is then sent to a computer using a universal serial bus (USB). b) Signal amplifications using the AFE. In the first stage (Gain 1), both the AC and DC parts are amplified, whereas in the second stage (Gain 2) only the AC part of the signal is amplified. c) Pulse signal from green, red, and NIR PLEDs for different PLED current densities. Current densities of 1, 2, 4, and 10 mA cm^{-2} are used for all the PLEDs. The bars show the pulse signal magnitudes (the error bars represent the standard deviation of the data collected for three separate runs). At 10 mA cm^{-2} current density, reproducible pulse signals are obtained from all the three colors. d–f) PPG signal and detected heartbeat peaks from the PPG signal from green, red, and NIR PLEDs, respectively at 10 mA cm^{-2} current density. The top panels show the PPG signal, and the bottom panels show the detected heartbeats using a peak detection algorithm.

the heartbeat peaks is shown in Figure 5b (black trace). In pulse oximetry, the ratios of the PPG signals are used to calculate the ratio of the PPG signal obtained from two separate channels, $R_{os} = \frac{Rd_{AC}/Rd_{DC}}{Gr_{AC}/Gr_{DC}}$ (Figure 5b orange trace). The arterial oxygen saturation, S_aO_2, is then derived from R_{os} and the molar extinction coefficient of oxyhemoglobin ($\varepsilon_{\lambda,HbO_2}$) and deoxyhemoglobin ($\varepsilon_{\lambda,Hb}$) at each wavelength:

$$S_aO_2(R_{os}) = \frac{\varepsilon_{Rd,Hb} - \varepsilon_{Gr,Hb}R_{os}}{(\varepsilon_{Rd,Hb} - \varepsilon_{Rd,HbO_2}) + (\varepsilon_{Gr,HbO_2} - \varepsilon_{Gr,Hb})R_{os}} \quad (1)$$

We calculated the oxygen saturation obtained by the pulse oximeter (S_pO_2) (bottom panel of Figure 5b) using an empirical correction to Beer–Lambert's law. We recorded an average oxygen saturation S_pO_2 of 98.77% which is verified using a commercially available transmission-mode pulse oximeter (Figure S7, Supporting Information).

In conclusion, in this work, we have introduced a surface-energy-patterning (SEP) technique to fabricate stable and reproducible PLEDs by blade coating. Three different colors, green, red, and NIR, are fabricated and their light-emitting characteristics are presented in detail. The use of SEP greatly improved the reproducibility of the devices, reduced the amount of solution used, and resulted in uniform film thicknesses. By utilizing SEP to coat two different PLEDs, we have successfully demonstrated multicolor blade-coated PLEDs on the same flexible substrate. Additionally, to apply the multicolor PLEDs as light sources for optical sensors, we found optimum operating conditions for each PLED to obtain adequate PPG signal levels. As a system-level implementation, multicolor PLEDs

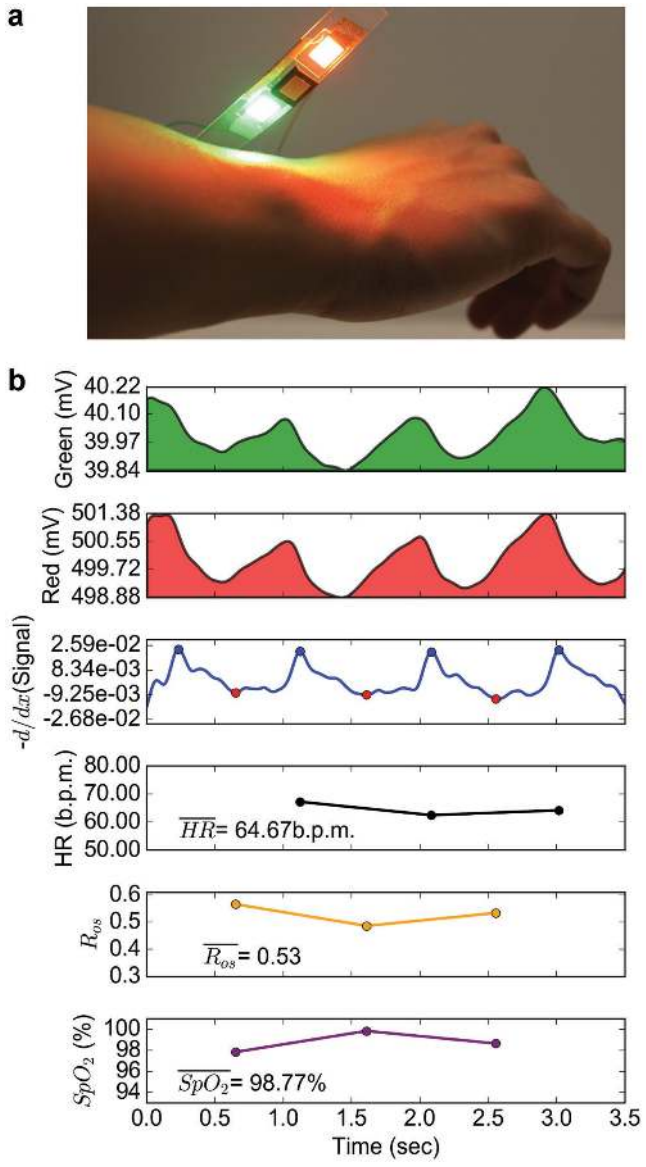

Figure 5. Reflection-mode pulse oximetry using green and red PLEDs, and a silicon PD on a volunteer's wrist. a) Photograph of the optoelectronic sensor that uses green and red PLEDs as the light source and a silicon PD as the light detector (the sensor is placed on top of the wrist for collecting the PPG signal). b) Reflection-mode pulse oximetry results. The top two panels (green and red) show the PPG signal from the green and red PLEDs, respectively. Panel 3 shows heartbeat peaks (blue dots) and valleys (red dots) detected from the PPG signals. Panel 4 shows the detected heart rate (HR) in beats per minute (b.p.m.) by timing the heartbeat peaks (blue dots in panel 3). The ratio of the red and green signals, R_{OS} and calculated oxygen saturation S_pO_2 are shown in the bottom two panels using orange and purple colors, respectively. Average oxygen saturation S_pO_2 of 98.77% is observed using an empirical correction to Beer–Lambert's law.

(green and red) in conjunction with a silicon photodiode are used to successfully perform PPG and oxygenation measurements. We hope that the demonstrations and findings presented in this paper will provide useful knowledge and encourage more research on printed PLEDs. Also, we hope that this result will stretch the OLED application boundary beyond the display domain to novel sensing applications, where the low-cost large-area benefits of PLEDs are fully utilized.

Experimental Section

Substrate Preparation: 125 µm thick PEN film precoated with a 3 µm planarization layer was laminated on 35 cm × 35 cm glass carrier substrate using a clear adhesive gel-film to give rigidity during processing. A 65 nm ITO layer was deposited via magnetron sputtering in vacuum on top of the substrates which were then patterned using photolithography. The result stack of glass carrier, adhesive, and PEN with patterned ITO were then covered with peelable protection film and scribed to 10 cm × 10 cm substrates. The PEN/ITO substrate was rinsed with ethanol before it was baked in the vacuum hotplate at 80 °C overnight. The substrate was taken out in the ambient air and heated up on a hotplate at 180 °C for 30 min. Then the substrate was treated with plasma for 10 s and entire surface was treated with (heptadecafluoro-1,1,2,2-tetrahydrodecyl)trichlorosilane (Gelest SIH5841.0) for 20 min under light vacuum (0.1–1 Torr).

Blade-Coater Setup: A doctor blade (Zehntner ZUA 2000.60) was used to coat PEDOT:PSS (Clevios AI4083, Heraeus), EBL, and the emissive layer. Two linear actuators (Servo City) were set up inside and outside a glovebox, heights of which were adjusted to coat on the substrate placed on a hotplate.

Thickness Measurement: Substrates were firmly mounted on a glass/Gel-Film system. A Dektak profiler (Veeco 6M) was used to measure the film thickness.

PLED Fabrication: SEP was done by masking the substrate with Kapton tape before it was plasma treated for 90 s. 75 µL of PEDOT:PSS was blade-coated with a blade height of 50 µm at 1 cm^{-1} on a hotplate set to 90 °C. The temperature of the hotplate was increased to 130 °C right after blade coating and the substrate was annealed at that temperature for 10 min. Then the sample was moved inside the glovebox and EBL was blade-coated with a 50 µL of solution, blade height of 50 µm at 1 cm s^{-1} on a hotplate set to 65 °C. One example of such EBL is poly(9,9-dioctylfluorene-*co*-*N*-(4-butylphenyl)-diphenylamine) (TFB).[1] After the coat, hotplate was set to 180 °C for 60 min. After annealing, the hotplate was set to 65 °C again and the emissive layer was blade-coated with 50 µL of solution, 200 µm blade height at 2 cm^{-1}. A green-emissive layer that can be used is poly((9,9-dioctylfluorene-2,7-diyl)-*alt*-(2,1,3-benzothiadiazole-4,8-diyl)) (F8BT) blended with TFB, and mixture of F8BT, TFB, and poly((9,9-dioctylfluorene-2,7-diyl)-*alt*-(4,7bis(3-hexylthiophene-5-yl)-2,1,3-benzothiadiazole)-2′,2′-diyl) for red.[1] The film was annealed at 140 °C for 10 min. The sample was transferred into a thermal evaporator for deposition of calcium (99.5%, STREM CHEMICALS) and aluminum (99.999%, ACI ALLOYS INC).

Device Encapsulation: A drop of UV curable epoxy was placed on top of an active pixel and pressed gently with a precut plastic film (PQA1). The sample was placed under UV radiation with a UV lamp (BHK INC.)

Device Characterization: The fabricated devices were measured using Keithley 2601 and Keithley 2400 to characterize for *J*–*V* and to take photodiode readings, respectively. Emission spectra and total flux were measured using Keithley 2601 and a spectrometer (SP-75, Orboptronix) equipped with an integrating sphere.

Reflection-Mode Oximeter Data Acquisition, Processing, and Interpretation: The reflection-mode oximeter system was composed of a Texas Instruments MSP430 µC and an analog front end (AFE4490). The AFE controlled the PLEDs and the PD (Hamamatsu S2387-66R), and allowed software control of the PLED drive current and gain parameters of the PD current read circuit. A 100 kΩ resistor (first stage) and 3 dB (second stage) gain were used for amplifying the PD signal. The AFE was interfaced to the µC over SPI bus, and the final processed signal from the µC was sent to a computer using a USB. Heart rate was calculated from the PPG signal using a peak detection algorithm and

by timing the systolic peaks. Oxygenation was calculated by obtaining the ratio of the red and green PPG signals, $R_{OS} = \frac{Rd_{AC}/Rd_{DC}}{Gr_{AC}/Gr_{DC}} \cdot R_{OS}$ was then used to calculate oxygen saturation, S_aO_2 using an empirical correction to Beer–Lambert's law. Reflection-mode oximetry experiments performed on human subjects were carried out with informed consent under the approval of the University of California, Berkeley Institutional Review Board, protocol ID number 2014-03-6081.

Supporting Information

Supporting Information is available from the Wiley Online Library or from the author.

Acknowledgements

This work was supported in part by Cambridge Display Technology Limited (CDT, Company Number 2672530), Systems on Nanoscale Information fabriCs (SONIC), one of the six SRC STARnet Centers, sponsored by MARCO and DARPA, and Intel Corporation via Semiconductor Research Corporation Grant No. 2014-IN-2571. The authors thank CDT for supplying OLED materials, Dr. Sangwan Kim, Adrien Pierre, and Xingchun Wang for helpful technical discussions.

Conflict of Interest

The authors declare no conflict of interest.

Keywords

blade coating, flexible electronics, polymer light-emitting diodes (PLEDs), printed sensors, pulse oximetry, organic light-emitting diodes (OLEDs), wearable sensors

Received: November 17, 2016
Revised: February 27, 2017
Published online:

[1] C. M. Lochner, Y. Khan, A. Pierre, A. C. Arias, *Nat. Commun.* **2014**, *5*, 5745.
[2] T. Yokota, P. Zalar, M. Kaltenbrunner, H. Jinno, N. Matsuhisa, H. Kitanosako, Y. Tachibana, W. Yukita, M. Koizumi, T. Someya, *Sci. Adv.* **2016**, *2*, e1501856.
[3] Y. Khan, A. E. Ostfeld, C. M. Lochner, A. Pierre, A. C. Arias, *Adv. Mater.* **2016**, *28*, 4373.
[4] M. S. White, M. Kaltenbrunner, E. D. Głowacki, K. Gutnichenko, G. Kettlgruber, I. Graz, S. Aazou, C. Ulbricht, D. A. M. Egbe, M. C. Miron, Z. Major, M. C. Scharber, T. Sekitani, T. Someya, S. Bauer, N. S. Sariciftci, *Nat. Photonics* **2013**, *7*, 811.
[5] B.-J. de Gans, P. C. Duineveld, U. S. Schubert, *Adv. Mater.* **2004**, *16*, 203.
[6] A. C. Arias, J. D. MacKenzie, I. McCulloch, J. Rivnay, A. Salleo, *Chem. Rev.* **2010**, *110*, 3.
[7] Y. Khan, F. J. Pavinatto, M. C. Lin, A. Liao, S. L. Swisher, K. Mann, V. Subramanian, M. M. Maharbiz, A. C. Arias, *Adv. Funct. Mater.* **2016**, *26*, 1004.
[8] J. R. Corea, A. M. Flynn, B. Lechêne, G. Scott, G. D. Reed, P. J. Shin, M. Lustig, A. C. Arias, *Nat. Commun.* **2016**, *7*, 10839.
[9] S. L. Swisher, M. C. Lin, A. Liao, E. J. Leeflang, Y. Khan, F. J. Pavinatto, K. Mann, A. Naujokas, D. Young, S. Roy, M. R. Harrison, A. C. Arias, V. Subramanian, M. M. Maharbiz, *Nat. Commun.* **2015**, *6*, 6575.
[10] Y. Khan, M. Garg, Q. Gui, M. Schadt, A. Gaikwad, D. Han, N. A. D. Yamamoto, P. Hart, R. Welte, W. Wilson, S. Czarnecki, M. Poliks, Z. Jin, K. Ghose, F. Egitto, J. Turner, A. C. Arias, *Adv. Funct. Mater.* **2016**, *26*, 8764.
[11] J. Bharathan, Y. Yang, *Appl. Phys. Lett.* **1998**, *72*, 2660.
[12] F. C. Krebs, *Sol. Energy Mater. Sol.* **2009**, *93*, 465.
[13] A. Sandström, H. F. Dam, F. C. Krebs, L. Edman, *Nat. Commun.* **2012**, *31002*.
[14] J. Birnstock, J. Blässing, A. Hunze, M. Scheffel, M. Stößel, K. Heuser, G. Wittmann, J. Wörle, A. Winnacker, *Appl. Phys. Lett.* **2001**, *78*, 3905.
[15] P. Kopola, M. Tuomikoski, R. Suhonen, A. Maaninen, *Thin Solid Films* **2009**, *517*, 5757.
[16] S.-R. Tseng, H.-F. Meng, K.-C. Lee, S.-F. Horng, *Appl. Phys. Lett.* **2008**, *93*, 153308.
[17] C.-Y. Chen, H.-W. Chang, Y.-F. Chang, B.-J. Chang, Y.-S. Lin, P.-S. Jian, H.-C. Yeh, H.-T. Chien, E.-C. Chen, Y.-C. Chao, H.-F. Meng, H.-W. Zan, H.-W. Lin, S.-F. Horng, Y.-J. Cheng, F.-W. Yen, I-F. Lin, H.-Y. Yang, K.-J. Huang, M.-R. Tseng, *J. Appl. Phys.* **2011**, *110*, 094501.
[18] H. Youn, K. Jeon, S. Shin, M. Yang, *Org. Electron.* **2012**, *13*, 1470.
[19] A. Pierre, M. Sadeghi, M. M. Payne, A. Facchetti, J. E. Anthony, A. C. Arias, *Adv. Mater.* **2014**, *26*, 5722.
[20] A. Pierre, I. Deckman, P. B. Lechêne, A. C. Arias, *Adv. Mater.* **2015**, *27*, 6411.
[21] Q. Sun, Y. A. Wang, L. S. Li, D. Wang, T. Zhu, J. Xu, C. Yang, Y. Li, *Nat. Photonics* **2007**, *1*, 717.
[22] F. Maier-Flaig, J. Rinck, M. Stephan, T. Bocksrocker, M. Bruns, C. Kübel, A. K. Powell, G. A. Ozin, U. Lemmer, *Nano Lett.* **2013**, *13*, 475.
[23] P.-Y. Chen, C.-L. Chen, C.-C. Chen, L. Tsai, H.-C. Ting, L.-F. Lin, C.-C. Chen, C.-Y. Chen, L.-H. Chang, T.-H. Shih, Y.-H. Chen, J.-C. Huang, M.-Y. Lai, C.-M. Hsu, Y. Lin, *SID Symp. Dig. Tech. Pap.* **2014**, *45*, 396.
[24] J. G. Webster, *Design of Pulse Oximeters*, CRC Press, Boca Raton, FL, USA **1997**.
[25] B. Chance, M. Cope, E. Gratton, N. Ramanujam, B. Tromberg, *Rev. Sci. Instrum.* **1998**, *69*, 3457.